Correspondence to:
J. Yue,
jia.yue@hamptonu.edu

Increasing carbon dioxide concentration in the upper atmosphere observed by SABER

Jia Yue[1], James Russell III[1], Yongxiao Jian[1], Ladislav Rezac[1,2], Rolando Garcia[3], Manuel López-Puertas[4], and Martin G. Mlynczak[5]

[1]Center for Atmospheric Science, Hampton University, Hampton, Virginia, USA, [2]Max Planck Institute for Solar System Research, Göttingen, Germany, [3]National Center for Atmospheric Research, Boulder, Colorado, USA, [4]Instituto de Astrofísica de Andalucía, CSIC, Granada, Spain, [5]NASA Langley Research Center, Hampton, Virginia, USA

Abstract Carbon dioxide measurements made by the Sounding of the Atmosphere using Broadband Emission Radiometry (SABER) instrument between 2002 and 2014 were analyzed to reveal the rate of increase of CO_2 in the mesosphere and lower thermosphere. The CO_2 data show a trend of ~5% per decade at ~80 km and below, in good agreement with the tropospheric trend observed at Mauna Loa. Above 80 km, the SABER CO_2 trend is larger than in the lower atmosphere, reaching ~12% per decade at 110 km. The large relative trend in the upper atmosphere is consistent with results from the Atmospheric Chemistry Experiment Fourier Transform Spectrometer (ACE-FTS). On the other hand, the CO_2 trend deduced from the Whole Atmosphere Community Climate Model remains close to 5% everywhere. The spatial coverage of the SABER instrument allows us to analyze the CO_2 trend as a function of latitude for the first time. The trend is larger in the Northern Hemisphere than in the Southern Hemisphere mesopause above 80 km. The agreement between SABER and ACE-FTS suggests that the rate of increase of CO_2 in the upper atmosphere over the past 13 years is considerably larger than can be explained by chemistry-climate models.

1. Introduction

Carbon dioxide (CO_2) has been constantly rising owing to human activities in the industrial age, mainly fossil fuel combustion and deforestation [e.g., *Keeling et al.*, 1976]. Because CO_2 is chemically stable and can exist in the atmosphere for a very long time [*Solomon et al.*, 2009], it can alter the radiative forcing of Earth's climate, leading to warming at the surface [*Intergovernmental Panel on Climate Change*, 2007]. The annual mean growth rate of CO_2 at Mauna Loa Observatory, Hawaii, during 2000–2014 is about 5% per decade (for example, http://www.esrl.noaa.gov/gmd/ccgg/trends/).

CO_2 is well mixed up to the upper mesosphere, where its mixing ratio falls off due to molecular diffusive separation and photolysis [e.g., *Lopez-Puertas et al.*, 2000; *Garcia et al.*, 2014; *Rezac et al.*, 2015, and references therein]. Thus, anthropogenic increases in CO_2 are expected to propagate upward up to the lower thermosphere. Contrary to the well-known greenhouse effect in the troposphere, CO_2 generally produces infrared radiative cooling above the tropopause [*Roble and Dickinson*, 1989; *Mlynczak et al.*, 1999a, 1999b; *Lopez-Puertas et al.*, 2000]. Presumably as a consequence of CO_2 cooling and downward heat conduction, the thermospheric density derived from satellite orbits has been decreasing for decades [*Emmert et al.*, 2008]. In order to understand secular changes in Earth's upper atmosphere, it is crucial to measure the CO_2 abundance in that region and to monitor its long-term change [*Qian et al.*, 2011]. Because most of the previous rocket or satellite CO_2 measurements in the upper atmosphere had a rather short duration and limited spatial coverage [*Lopez-Puertas et al.*, 2000], there is a compelling need to monitor the CO_2 trend in the upper atmosphere using long-duration satellite observations. *Emmert et al.* [2012] reported the increase of CO_x (the sum of CO_2 and CO) in the mesosphere and lower thermosphere (MLT) between 2004 and 2012 using solar occultation data obtained by the Atmospheric Chemistry Experiment Fourier Transform Spectrometer (ACE-FTS) on board the SCISCAT-1 satellite [*Bernath et al.*, 2005; *Beagley et al.*, 2010; *Foucher et al.*, 2011]. The measured global increase rate of 8–9% per decade at ~100 km was, surprisingly, much faster than the 5% per decade predicted by a global-average 1-D model [*Roble*, 1995]. Increasing vertical mixing in the MLT in the 1-D model produced better agreement with ACE-FTS observations, leading Emmert et al. to suggest an increasing trend in vertical diffusion as a possible cause of the large rate of increase of CO_2 observed in the upper atmosphere.
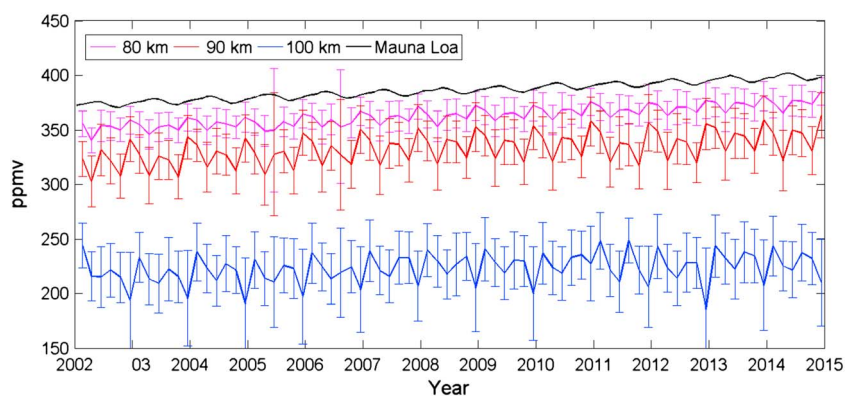
Figure 1. Time series of SABER CO_2 VMR averaged over 60 days (the SABER yaw cycle) and over the latitude range ±54° at 80 km (pink), 90 km (red), and 100 km (blue). The time series of CO_2 measured at Mauna Loa Observatory is denoted in black. The uncertainty is the 2σ standard deviation of the VMR data within 60 day periods.

An independent, longer, and more extensive satellite record of CO_2 volume mixing ratio (VMR) is desired to compare with the result of *Emmert et al.* [2012]. Two years prior to the SCISCAT-1 launch, on 7 December 2001, the Sounding of the Atmosphere using Broadband Emission Radiometry (SABER) instrument was launched on the Thermosphere Ionosphere Mesosphere Energetics and Dynamics (TIMED) satellite [*Russell et al.*, 1999]. Both SABER and TIMED are still operating normally to date. The SABER CO_2 VMR data set recently became available at http://saber.gats-inc.com/ [*Rezac et al.*, 2015]. The SABER CO_2 data coverage extends from 2002 to the present, or about 2 years longer than the contemporary ACE-FTS CO_2 data. Unlike the solar occultation measurement of the ACE-FTS, the SABER CO_2 VMR is obtained from limb infrared emission measurements and allows for more complete latitude coverage. An inversion algorithm has been applied to all the daytime measurements resulting in more than 1 million CO_2 VMR profiles, as compared to ~26,500 ACE-FTS profiles used in *Emmert et al.* [2012]. More importantly, SABER has continuous and nearly homogeneous latitude/longitude coverage at low and middle latitudes (±54°). Latitude coverage varies with time because TIMED performs a yaw maneuver approximately every 60 days such that the SABER detector does not face the Sun directly; this yields latitudinal coverage of 54°S–83°N and 54°N–83°S on alternate yaw cycles. In this paper, we present the long-term trend derived from SABER CO_2 VMR measurements in the MLT from 2002 to 2014. The observed trend is compared to that predicted by the National Center for Atmospheric Research (NCAR) Specified Dynamics Whole Atmosphere Climate Community Model (SD-WACCM) and to the ACE-FTS trend.

2. Observations

A two-channel algorithm (4.3 μm and 15 μm narrow band) is used to simultaneously retrieve profiles of kinetic temperature T_k and CO_2 VMR from SABER daytime radiances observed over the period from 2002 to 2014 [*Rezac et al.*, 2015]. The uncertainty of retrieved CO_2 VMR profiles is 15% at 80 km, reaches a minimum around 90 km (12%) and grows again to 32% at 110 km [*Rezac et al.*, 2015]. The predominant uncertainties come from nonlocal thermodynamic equilibrium modeling parameters and the density of the CO_2 collisional partners. The annual mean SABER CO_2 profile is consistent with previous satellite and rocket observations. As noted earlier, CO_2 departs from the well-mixed state at ~ 80 km, due principally to molecular diffusive separation.

Figure 1 displays the time series of CO_2 abundance at 80 km, 90 km, and 100 km from February 2002 to December 2014 averaged over the latitudes ±54°. We bin the data every 60 days (one yaw cycle). Note that among the CO_2 VMR uncertainties [*Rezac et al.*, 2015], the collisional rate coefficients have no trends. Above ~95 km, the O and O^1D used in the SABER CO_2 retrieval are from WACCM [*Rezac et al.*, 2015]. WACCM atomic oxygen shows a nearly zero long-term trend in the region where it is important for the inversion of CO_2 above ~100 km. Via ionospheric measurements and satellite drag data, *Danilov* [2015] and *Emmert* [2015] speculate that there might be a negative trend in O to account for the observed trends in the thermospheric density and ionospheric parameters. But to our best knowledge, no significant trends have been observed in O and O^1D in the upper atmosphere. Assuming that O has a positive trend of 5% per decade would lead
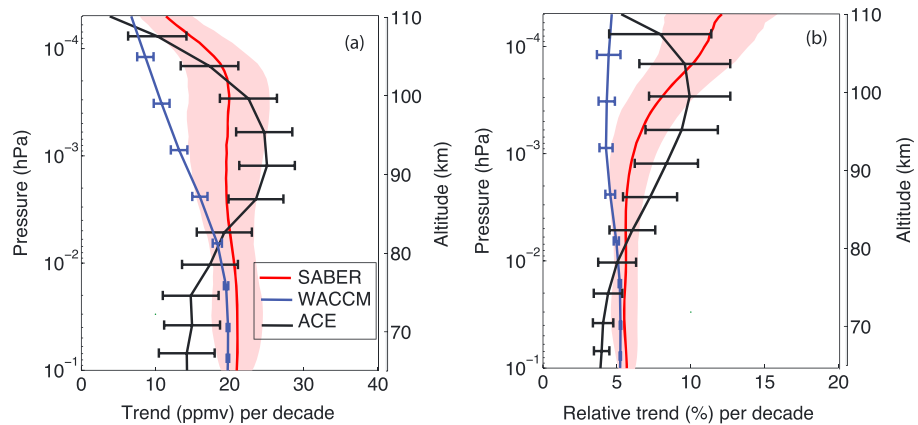
Figure 2. Vertical profiles of (a) absolute trends of CO_2 VMR (ppmv per decade) obtained from SABER (red) and ACE-FTS (black) and (b) relative trends (% per decade). The SD-WACCM trend is in blue. Shaded areas and cross bars denote the uncertainty of the regression analysis. Uncertainties are 2σ.

to ~1–1.5% per decade positive trend in CO_2 retrieval; that is, our derived CO_2 trend would then be 1–1.5% smaller. In the case of a negative O trend, *Emmert* [2015] inferred a -2.6%/decade O trend during 1967–2013 (see his Table 2), with this decrease rate our derived CO_2 trend would be 1% larger at most. Therefore, in this paper, the O and O^1D trends are not considered in the CO_2 trend uncertainty. In addition, the random instrument noise of 1–2% is much smaller than the variance of the observations. Thus, the error bars in Figure 1 are the 2σ standard deviation of the VMR representing the geophysical variance of the data within each 60 day yaw cycle. The uncertainty of the CO_2 retrieval (the uncertainty of the mean) is not considered. As shown in Figure 1, CO_2 is increasing monotonically at all levels in the upper atmosphere, although not at the same rate as in the Mauna Loa measurements, as we shall see below.

The CO_2 VMR trend in the MLT, as well as other interannual oscillations such as the solar cycle and the quasi-biennial oscillation (QBO) can be estimated from the SABER CO_2 deseasonalized residual by multiple linear regression (MLR). The regression equation used to calculate the CO_2 trend is

$$CO_2(t) = \mu + \alpha \cdot t + \beta \cdot QBO(t) + \gamma \cdot solar(t) \tag{1}$$

In this MLR, the long-term trend, and the dependence on the QBO and the solar cycle are considered. The QBO and 11 year solar cycle are represented by the 30 mb zonal mean zonal wind at the equator and the 10.7 cm radio flux [*Tapping*, 2013], respectively [*Stolarski et al.*, 1991; *Li et al.*, 2013]. The quantity μ represents a constant CO_2 mixing ratio. The MLR uncertainty of the trend depends on the scatter of the residuals [*Randel and Cobb*, 1994; *Li et al.*, 2013] and is modified by taking into account their autocorrelation. The temporal resolution of the SABER time series is 60 days, which corresponds to the binning of the data in each yaw cycle.

The linear trend of SABER CO_2 VMR at 80 km is 20.6 ± 3.0 ppmv or ~5% per decade (uncertainties are 2σ). This is consistent with the Mauna Loa trend of ~20.5 ppmv per decade or 5% from 2000 to 2014, denoted by the black curve in Figure 1. Because the CO_2 VMR falls off from a constant value around 80 km, the absolute trends at 90 km (~0.01 hPa), 100 km, and 110 km are smaller: 19.5 ± 4.5, 19.9 ± 5.5, and 12.8 ± 3.7 ppmv per decade, respectively. The SABER CO_2 VMR trend at 100 km is comparable to the ACE-FTS trend of 23.5 ± 6.3 ppmv per decade within the uncertainties [*Emmert et al.*, 2012]. The CO_2 responses to the solar cycle and the QBO have also been calculated from the MLR and will be reported in a future paper.

We show in Figure 2, the absolute and relative SABER CO_2 trend vertical profiles calculated from data averaged over ±54° latitude, along with their uncertainties derived from the MLR method. The relative trend is computed by dividing the absolute trend by the time mean CO_2 VMR between 2002 and 2014. Note that each trend is relative to the time mean CO_2 VMR from its own data set. For comparison, the CO_2 trend calculated with SD-WACCM from 2002 to 2012 is also shown. SD-WACCM is a general circulation model extending from the ground to the thermosphere that includes chemistry, dynamics, and energetics [*Marsh et al.*, 2013, and references therein]. Surface mixing ratios of CO_2 are specified from global ground observations. SD-WACCM
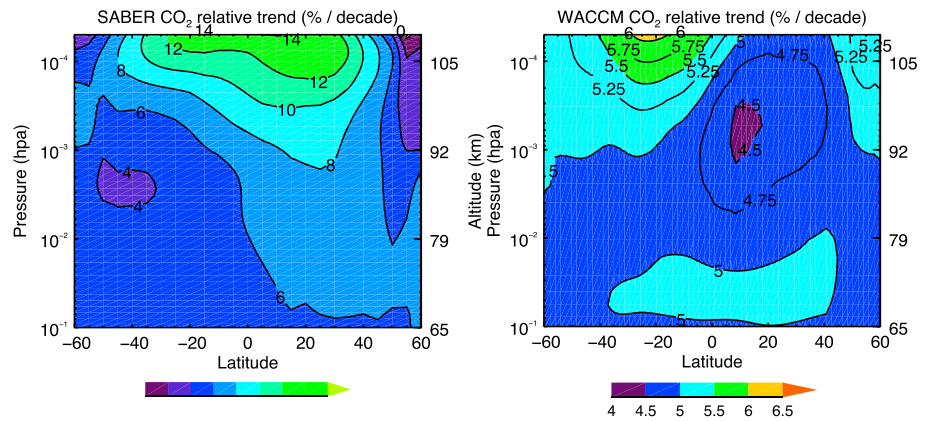
Figure 3. (left) SABER and (right) SD-WACCM CO_2 relative trends (% per decade) as functions of latitude and height. The color scales and contour intervals are different for the SABER and WACCM plots.

is constrained by Modern Era Retrospective Analysis for Research and Applications (MERRA) in the troposphere and stratosphere. *Garcia et al.* [2014] show good agreement between the SD-WACCM simulation and ACE-FTS CO_2 climatology. The monthly mean SD-WACCM outputs from January 2002 to November 2012 within the latitudes of ±60° were analyzed by the same MLR as the SABER data. However, the SABER trend is computed for daytime-only CO_2 because no nighttime retrievals are currently available, while SD-WACCM simulates the full diurnal cycle. *Emmert et al.* [2012] suggested that there is no significant local time dependence to the trends, as they found no differences in the trend derived from sunrise and sunset separately. Thus, we assume that there is no significant difference between daytime and nighttime CO_2 trends.

Figure 2a shows that the absolute SD-WACCM CO_2 trend falls off along with the mean CO_2 VMR above 10^{-2} hPa (~80 km). On the contrary, the SABER CO_2 trend remains nearly constant at 20 ppmv per decade and falls off only above 10^{-4} hPa (~110 km). The observed trend is about 10 ppmv per decade larger than that derived from SD-WACCM at 110 km. In Figure 2b, SD-WACCM shows a vertically uniform relative trend of about 5% per decade, which is similar to the trend from the 1-D global mean model considered by *Emmert et al.* [2012], and reflects the anthropogenic increase of CO_2 in the lower atmosphere. On the other hand, SABER detects a larger trend of up to 12% per decade at 2×10^{-5} hPa (~110 km). The SABER CO_2 trend provides support for the ACE-FTS CO_2 trend reported in *Emmert et al.* [2012]. Figure 2b also shows our analysis of ACE-FTS data between 2004 and 2014 (all latitudes are included and deseasonalized), the same as in *Emmert et al.* [2012]. The ACE CO_2 relative trend profile reaches a peak of ~10% near 105 km. Note that the ACE trend is smaller than the Mauna Loa or the SABER trend below 80 km in Figure 2. This is because an a priori stratospheric trend is used in ACE, which is too low for the period under study (i.e., after 2004). According to *Emmert et al.* [2012], this has no influence on the ACE trend above 90 km. In general, the ACE-FTS and SABER trends are consistent with each other within uncertainties, although the ACE trend peaks near 100 km, whereas the SABER trend continues to increase up to 110 km, the highest altitude at which data are available.

We also derived the SABER CO_2 trend as a function of latitude, and the results are shown in Figure 3a. In the MLT region (90–110 km), the SABER CO_2 trend in the Northern Hemisphere is larger than 10% per decade, which is about 50% more than that in the Southern Hemisphere at the mesopause (~90 km). The SD-WACCM result shows the opposite hemispheric asymmetry, with a larger trend in the Southern Hemisphere, as shown in Figure 3b; furthermore, the hemispheric asymmetry in WACCM is slight compared to SABER in absolute values. In terms of relative values between two hemispheres, WACCM shows a hemispheric asymmetry of 20%.

3. Discussion and Summary

This paper has presented the first analysis of CO_2 trends derived from SABER data. It contains the longest CO_2 time series in existence (2002–2014) for the upper atmosphere, with more data to become available as long

as the instrument and satellite continue to operate normally. SD-WACCM and *Roble's* [1995] 1-D model predict a constant trend of about 5%; on the contrary, both the SABER and ACE-FTS CO_2 trends increase with altitude above ~80 km and reach 10–12% in the lower thermosphere. SABER infrared limb sounding and ACE-FTS solar occultation measurements complement each other in several aspects. ACE-FTS measurements occurred around sunrise and sunset with relatively sparse latitude coverage, while SABER CO_2, although currently available only in daytime, provides more uniform latitude coverage and more dense, homogeneous, and regular temporal coverage. These two satellite instruments measured a similar CO_2 trend profile despite their vastly different remote sensing techniques and temporal and spatial coverage. This lends support to the results from both sets of observations and suggests that they arise from a real physical cause instead of being due to uncertainties in the measurements or in the calculation of trends from relatively short data records.

To account for the discrepancy between the model and observed CO_2 trend, *Emmert et al.* [2012] suggested the possibility of a positive trend in vertical mixing. If the eddy diffusion coefficient K_{zz} is increased by 15% per decade in Roble's 1-D model, the calculated CO_2 trend is closer to the ACE-FTS observed trend [*Emmert et al.*, 2012]. SD-WACCM is a comprehensive chemistry-climate model; however, small-scale gravity waves cannot be explicitly resolved, and their effects must be parameterized [*Richter et al.*, 2010]. In SD-WACCM simulations for the period in question, no significant trend in K_{zz} is calculated (R. Garcia, private communication, 2015). Although there are a few localized observations suggesting that gravity wave fluxes may be increasing [*Hoffmann et al.*, 2011], there is no conclusive evidence for global trends in gravity waves and eddy diffusion.

There is at present no plausible hypothesis to explain the hemispheric asymmetry in the SABER CO_2 trend (Figure 3). Although it is well known that tropospheric CO_2 emission is greater in the Northern Hemisphere than in the Southern Hemisphere, this asymmetry becomes negligible in the upper troposphere and stratosphere [*Hall and Prather*, 1993]. If we assume that changes in gravity wave activity lead to changes in eddy diffusion, the behavior of the SABER CO_2 trend could be explained if diffusion due to gravity waves is increasing more rapidly in the Northern Hemisphere. A different rate of increase of gravity wave activity in the two hemispheres has not been observed or simulated by models. Moreover, interhemispheric asymmetry largely disappears in WACCM when trends are calculated over longer periods (not shown). There are two possible reasons for this: (1) WACCM contains stochastic, low-frequency interannual variability in dynamics and transport, such that different trends are obtained over different short periods; (2) when the MLR is performed using a short period, the MLR procedure has difficulty allocating variance accurately between the trend and the 11 year solar cycle, whereas a longer period of analysis yields much more robust results. Be that as it may, we emphasize that WACCM fails to reproduce the large trends in CO_2 above 10^{-3} hPa seen in SABER and ACE data.

In this paper, we have reported the rate of increase of CO_2 from the two-channel retrieved SABER data set. The CO_2 trend below 80 km of ~5% per decade is similar to that measured at Mauna Loa Observatory at the surface. SABER and ACE-FTS CO_2 shows a faster increase rate above 80 km, compared to SD-WACCM or any current models that we are aware of (e.g., NCAR 1-D model [*Emmert et al.*, 2012] and HAMMONIA (H. Schmidt, private communication, 2015). The SABER CO_2 trend shows a peak at ~110 km of about 12% per decade. The trend shows significant latitudinal and height dependence, with the Northern Hemisphere trend being larger than that in the Southern Hemisphere in the 10^{-2} to 10^{-4} hPa pressure range (~80 to 110 km).

References

Beagley, S. R., C. D. Boone, V. I. Fomichev, J. J. Jin, K. Semeniuk, J. C. McConnell, and P. F. Bernath (2010), First multi-year occultation observations of CO_2 in the MLT by ACE satellite: Observations and analysis using the extended CMAM, *Atmos. Chem. Phys.*, 10, 1133–1153.

Bernath, P. F., et al. (2005), Atmospheric Chemistry Experiment (ACE): Mission overview, *Geophys. Res. Lett.*, 32, L15S01, doi:10.1029/2005GLO22386.

Danilov, A. (2015), Seasonal and diurnal variations in f_oF2 trends, *J. Geophys. Res. Space Physics*, 120, 3868–3882, doi:10.1002/2014JA020971.

Emmert, J. T. (2015), Altitude and solar activity dependence of 1967–2005 thermospheric density trends derived from orbital drag, *J. Geophys. Res. Space Physics*, 120, 2940–2950, doi:10.1002/2015JA021047.

Emmert, J. T., J. M. Picone, and R. R. Meier (2008), Thermospheric global average density trends, 1967–2007, derived from orbits of 5000 near-Earth objects, *Geophys. Res. Lett.*, 35, L05101, doi:10.1029/2007GL032809.

Emmert, J. T., M. H. Stevens, P. F. Bernath, D. P. Drob, and C. D. Boone (2012), Observations of increasing carbon dioxide concentration in Earth's thermosphere, *Nat. Geosci.*, 5, 868–871, doi:10.1038/NGEO1626.

Foucher, P. Y., A. Chedin, R. Armante, C. Boone, C. Crevoisier, and P. Bernath (2011), Carbon dioxide atmospheric vertical profiles retrieved from space observation using ACE-FTS solar occultation instrument, *Atmos. Chem. Phys.*, 11, 2455–2470.

Garcia, R. R., M. López-Puertas, B. Funke, D. R. Marsh, D. E. Kinnison, A. K. Smith, and F. González-Galindo (2014), On the distribution of CO_2 and CO in the mesosphere and lower thermosphere, *J. Geophys. Res. Atmos.*, 119, 5700–5718, doi:10.1002/2013JD021208.

Hall, T. M., and M. J. Prather (1993), Simulations of the trend and annual cycle in the stratospheric CO_2, *J. Geophys. Res.*, 98(D6), 10,573–10,581, doi:10.1029/93JD00325.

Hoffmann, P., M. Rapp, W. Singer, and D. Keuer (2011), Trends of mesospheric gravity waves at northern middle latitudes during summer, *J. Geophys. Res.*, 116, D00P08, doi:10.1029/2011JD015717.

Intergovernmental Panel on Climate Change (2007), *Climate Change 2007: The Physical Science Basis. Contribution of Working Group I to the Fourth Assessment Report of the Intergovernmental Panel on Climate Change*, edited by S. Solomon et al., Cambridge Univ. Press, Cambridge, U. K., and New York.

Keeling, C. D., R. B. Bacastow, A. E. Bainbridge, C. A. Ekdahl, P. R. Guenther, L. S. Waterman, and J. F. S. Chin (1976), Atmospheric carbon dioxide variations at Mauna Loa Observatory, Hawaii, *Tellus*, 28, 538–551.

Li, T., N. Calvo, J. Yue, X. Dou, J. Russell, M. Mlynczak, C. Y. She, and X. Xue (2013), Influence of El Niño-Southern Oscillation in the mesosphere, *Geophys. Res. Lett.*, 40, 3292–3296, doi:10.1002/grl.50598.

Lopez-Puertas, M., M. A. Lopez-Valverde, R. R. Garcia, and R. G. Roble (2000), A review of CO_2 and CO abundance in the middle atmosphere, in *Atmospheric Science Across the Stratopause, Geophys. Monogr. Ser.*, vol. 123, edited by D. E. Siskind, S. D. Eckermann, and M. E. Summers, pp. 83–100, AGU, Washington, D. C.

Marsh, D. R., M. J. Mills, D. E. Kinnison, L. Jean-Francois, N. Calvo, and L. M. Polvani (2013), Climate change from 1850 to 2005 simulated in CESM1(WACCM), *J. Clim.*, 26, 7372–7391.

Mlynczak, M. G., C. J. Mertens, R. R. Garcia, and R. W. Portmann (1999a), A detailed evaluation of the stratospheric heat budget: 1. Radiation transfer, *J. Geophys. Res.*, 104(D6), 6021–6038, doi:10.1029/1998JD200100.

Mlynczak, M. G., C. J. Mertens, R. R. Garcia, and R. W. Portmann (1999b), A detailed evaluation of the stratospheric heat budget: 2. Global radiation balance and diabatic circulations, *J. Geophys. Res.*, 104(D6), 6039–6066, doi:10.1029/1998JD200099.

Qian, L., J. Laštovička, R. G. Roble, and S. C. Solomon (2011), Progress in observations and simulations of global change in the upper atmosphere, *J. Geophys. Res.*, 116, A00H03, doi:10.1029/2010JA016317.

Randel, W. J., and J. B. Cobb (1994), Coherent variations of monthly mean column ozone and lower stratospheric temperature, *J. Geophys. Res.*, 99(D3), 5433–5447, doi:10.1029/93JD03454.

Rezac, L., A. Kutepov, J. M. Russell III, A. G. Feofilov, J. Yue, and R. A. Goldberg (2015), Simultaneous retrieval of $T(p)$ and CO_2 VMR for non-LTE limb radiance measured by the SABER/TIMED instrument, *J. Atmos. Sol. Terr. Phys.*, 130–131, 23–42.

Richter, J. H., F. Sassi, and R. R. Garcia (2010), Toward a physically based gravity wave source parameterization in a general circulation model, *J. Atmos. Sci.*, 67, 136–156.

Roble, R. G. (1995), Energetics of the mesosphere and thermosphere, in *The Upper Mesosphere and Lower Thermosphere: A Review of Experiment and Theory, Geophys. Monogr. Ser.*, vol. 87, edited by R. M. Johnson and T. L. Killeen, pp. 1–21, AGU, Washington, D. C., doi:10.1029/GM087p0001.

Roble, R. G., and R. E. Dickinson (1989), How will changes in carbon dioxide and methane modify the mean structure of the mesosphere and thermosphere, *Geophy. Res. Lett.*, 16(12), 1441–1444, doi:10.1029/GL016i012p01441.

Russell, J. M., III, M. G. Mlynczak, L. L. Gordley, J. J. Tansock Jr., and R. W. Esplin (1999), Overview of the SABER experiment and preliminary calibration results, *SPIE Proc.*, 3756, 277–288, doi:10.1117/12.366382.

Solomon, S., G.-K. Plattner, R. Knutti, and P. Friedlingstein (2009), Irreversible climate change due to carbon dioxide emissions, *Proc. Natl. Acad. Sci. U.S.A.*, 106, 1704–1709.

Stolarski, R. S., P. Bloomfield, R. D. McPeters, and J. R. Herman (1991), Total ozone trends deduced from Nimbus 7 Toms data, *Geophys. Res. Lett.*, 18, 1015–1018, doi:10.1029/91GL01302.

Tapping, K. F. (2013), The 10.7 cm solar radio flux ($F_{10.7}$), *Space Weather*, 11, 394–406, doi:10.1002/swe.20064.